Journal of Hazardous Materials 192 (2011) 545–553

Contents lists available at ScienceDirect

Journal of Hazardous Materials

journal homepage: www.elsevier.com/locate/jhazmat

Reutilization of Cr-Y zeolite obtained by biosorption in the catalytic oxidation of volatile organic compounds

B. Silva[a,*], H. Figueiredo[a], V.P. Santos[b], M.F.R. Pereira[b], J.L. Figueiredo[b], A.E. Lewandowska[c], M.A. Bañares[c], I.C. Neves[d], T. Tavares[a]

[a] IBB – Institute for Biotechnology and Bioengineering, Centre of Biological Engineering, University of Minho, Campus de Gualtar, 4710-057 Braga, Portugal
[b] Laboratory of Catalysis and Materials (LCM), Associate Laboratory LSRE-LCM, Chemical Engineering Department, Faculty of Engineering, University of Porto, Rua Dr. Roberto Frias, 4200-465 Porto, Portugal
[c] Catalytic Spectroscopy Laboratory, Institute of Catalysis and Petrochemistry, CSIC, E-28049 Madrid, Spain
[d] Department of Chemistry, Centre of Chemistry, University of Minho, Campus de Gualtar, 4710-057 Braga, Portugal

ARTICLE INFO

Article history:
Received 17 March 2011
Received in revised form 13 May 2011
Accepted 16 May 2011
Available online 23 May 2011

Keywords:
VOC
Total oxidation
Cr-NaY
Ethyl acetate
Ethanol
Toluene

ABSTRACT

This work aims at the reutilization of a Cr-loaded NaY zeolite obtained by biorecovery of chromium from water as catalyst in the oxidation of volatile organic compounds (VOC). Cr-NaY catalysts were obtained after biosorption of Cr(VI) using a bacterium, *Arthrobacter viscosus*, supported on the zeolite. The biosorption experiments were conducted at different pH values in the range 1–4. The catalysts were characterized by several techniques, namely ICP-AES, SEM-EDS, XRD, XPS, Raman, H_2-TPR and N_2 adsorption. The zeolite obtained at pH 4 has the highest content of chromium, 0.9%, and was selected as the best catalyst for the oxidation of different VOC, namely ethyl acetate, ethanol and toluene. For all VOC tested, the catalyst with chromium showed higher activity and selectivity to CO_2, in comparison with the starting zeolite NaY. The presence of chromium shifted also the reaction pathways. In terms of selectivity to CO_2, the following sequence was observed: ethyl acetate > toluene > ethanol.

1. Introduction

Volatile organic compounds (VOC) are considered to be the most important class of air pollutants and are emitted from a variety of industrial processes and transportation activities. They include a wide range of compounds, such as oxygenates, aromatics and halogenated hydrocarbons [1]. The emission of VOC is of particular concern due to their high toxicity and their easiness of spreading through the atmosphere. The release of these harmful compounds into the atmosphere has widespread environmental implications and has been linked to the stratospheric ozone depletion, formation of ground level ozone, enhancement of global greenhouse and contribution to the acidification of rain [2,3]. With this respect, strict regulations on the environmental standards have been applied in several countries in order to reduce VOC emissions [4].

Among the different techniques for VOC emission abatement, catalytic oxidation is considered to be a promising solution as it can be efficiently applied in a wide range of inlet VOC concentrations and gas flow rates [5–13]. The catalytic process offers high destructive efficiency at lower operating temperatures than the required by thermal oxidation processes [14–17]. The commercial catalysts for oxidation of VOC can be classified into two main categories: supported noble metals [18–21] and transition metal oxides (bulk or supported forms) [22–25]. The catalysts based on noble metals, such as platinum and palladium are the most commonly used for the complete oxidation at low temperature. Although it is generally accepted that noble metal catalysts are more active than metal oxides, their susceptibility to poisoning [26,27], high cost and limited availability have been encouraging their replacement by low cost transition metals [8,15]. These catalysts present sufficient activity, although they are in general less active than noble metals at low temperatures. Nevertheless, in some cases, these catalysts show performances as high or higher than supported noble metal catalysts [28]. Among the transition metals, chromium is an interesting metal to be applied in catalytic oxidation reactions because of its multiple oxidation states. Chromium catalysts have been extensively studied in the oxidation of many pollutants namely propene [29], ethyl acetate [30] and methylene chloride [31].

It is well known that supports strongly affect the catalytic activity, particularly in oxidation reactions. The type of support used has a significant influence on metal dispersion. In recent years, the use of zeolites as supports or as catalysts for oxidation reactions,

* Corresponding author. Tel.: +351 253 604 410.
E-mail address: bsilva@deb.uminho.pt (B. Silva).

0304-3894/$ – see front matter © 2011 Elsevier B.V. All rights reserved.
doi:10.1016/j.jhazmat.2011.05.056

has gained particular interest [10,12,21,26,29,32]. The advantage of zeolite-based catalyst is that the active metal components can be exchanged with the compensating cations in the zeolite, achieving a better metal dispersion. In addition, zeolites possess size and shape features that allow its use as effective catalysts in several reactions [12,32].

In this work, a technology based on the reuse of Cr(VI), recovered by a biosorption process, as catalyst for oxidation reactions is proposed. As reported in previous work [33], a low-cost system combining the biosorption properties of a microorganism with the ion exchange properties of a zeolite was able to remove hexavalent chromium from contaminated water. After the biosorption process, Y zeolite loaded with Cr can be used as competitive and selective catalyst to be applied in catalytic oxidation of volatile organic compounds [34]. Therefore, Cr(VI) that is usually considered a xenobiotic pollutant, can be reused as a catalyst to be applied in the oxidation of persistent organic compounds, presenting a double environmental benefit. The aim of this study is the reutilization of the chromium-containing NaY zeolite obtained by biorecovery of chromium from water as catalyst in the oxidation of ethyl acetate, ethanol and toluene.

2. Experimental

2.1. Biosorption assays

The metal-loaded zeolite samples were obtained after biosorption experiments as reported in a previous work (not yet published). The experiments were performed with *Arthrobacter viscosus* supported on NaY zeolite, using different pH values (1, 2, 3 and 4). The biomass concentration and initial Cr(VI) concentration used were 5 g/L and 100 mg/L, respectively. Batch experiments were conducted in 250 mL Erlenmeyer flasks using 15 mL of the *A. viscosus* suspension previously prepared, 150 mL of a potassium dichromate solution and 1.0 g of NaY zeolite. The solution pH was regularly maintained at the desired pH value using H_2SO_4 or NaOH 1 M solutions. The Erlenmeyer flasks were kept at 28 °C, with moderate stirring, until the equilibrium was established. Samples were taken and analyzed for chromium quantification. The chromium ions were quantified by the spectroscopic method of 1,5-diphenylcarbazide [35].

2.2. Characterization procedures

Elemental chemical analyses were performed by inductively coupled plasma atomic emission spectrometry (ICP-AES), using a Philips ICP PU 7000 Spectrometer, after acid digestion of the samples.

The morphology of the zeolite samples after biosorption was evaluated by scanning electron microscopy (SEM), using a Leica Cambridge S360, equipped with an energy dispersive X-ray spectroscopy (EDS) system. Solid samples were coated with Au in vacuum to avoid surface charging using a Fisons Instruments SC502 sputter coater.

Powder X-ray diffraction (XRD) patterns were recorded using a Philips Analytical X-ray model PW1710 BASED diffractometer system. Scans were taken at room temperature, using Cu Kα radiation in a 2θ range between 5° and 70°.

X-ray photoelectron spectroscopy (XPS) analyses were obtained in a VG Scientific ESCALAB 250iXL spectrometer using a monochromatic Al-Kα radiation at 1486.92 eV. In order to correct possible deviations caused by electric charge of the samples, the C 1s line at 285.0 eV was taken as internal standard [36,37].

Temperature programmed reduction (TPR) experiments were performed in an AMI-200 (Altamira Instruments) apparatus. The sample (50 mg) was placed in a U-shaped quartz tube located inside an electrical furnace and subjected to a 10 °C/min heating rate from room temperature to 600 °C, under a mixture of 5% (v/v) H_2/He, at a total flow rate of 30 cm^3/min. The H_2 consumption was followed by a thermal conductivity detector (TCD) and by mass spectrometry (Dymaxion 200 amu, Ametek).

Raman spectra were run with a single monochromator Renishaw System-1000 microscope Raman equipped with a cooled CCD detector (−73 °C) and holographic super-Notch filter. The holographic Notch filter removes the elastic scattering while the Raman signal remains high. The powdery samples were excited with the 514 nm Ar^+ line; spectral resolution was ca. 3 cm^{-1} and spectrum acquisition consisted of 40 accumulations of 10 s. The power at the sample was 0.9 mW. The spectra were obtained under hydrated and dehydrated conditions in a hot stage (Linkam TS-1500). The catalysts were dehydrated in synthetic airflow at 500 °C at a rate of 10 °C/min. Raman spectrum of dehydrated sample was run at 500 °C and after cooling in synthetic air at room temperature.

The textural characterization of the catalysts was based on the N_2 adsorption isotherms, determined at −196 °C using a Quantachrome Instruments Nova 4200e apparatus. The samples were previously outgassed at 150 °C under vacuum. The micropore volumes were calculated by the t-method. Surface areas were calculated by applying the BET equation.

2.3. Catalytic tests

The catalytic tests were performed using similar conditions as reported by Bastos et al. [38]. The catalyst (50 mg) was pretreated in air flow at 400 °C for 1 h, and then cooled to room temperature. The catalytic oxidation of ethyl acetate, ethanol and toluene was performed under atmospheric pressure. The flow rate of the reacting stream was 150 cm^3/min (measured at room temperature and pressure), which corresponds to a space velocity of 16 000 h^{-1} (determined in terms of total bed volume), with a composition of 2000 mg_{carbon}/m^3 (500 ppm of ethyl acetate, 1000 ppm of ethanol and 286 ppm of toluene). A feed stream with a composition of 4000 mg_{carbon}/m^3 (1000 ppm of ethyl acetate) was also used for the oxidation of ethyl acetate. The temperature was increased at 2.5 °C/min between room temperature and 500 °C. A fixed-bed reactor was used, consisting of a U-shaped quartz tube of 6 mm internal diameter, placed inside a temperature controlled electrical furnace. Temperature in the reaction zone was measured by a K type thermocouple placed in the middle of the catalyst bed. In order to minimize the thermal effects, the catalyst was diluted with an inert (carborundum) having the same size as the catalyst particles, between 0.2 and 0.5 mm. The gas mixture at the reactor outlet was analyzed by a CO_2 non-dispersive infrared (NDIR) sensor Vaisala GMT220 and a total volatile organic compounds analyzer MiniRAE2000 (which has different sensitivity for each VOC). The reaction was carried out in two cycles of increasing and decreasing temperature. The conversion into CO_2 (X_{CO_2}) was calculated as $X_{CO_2} = F_{CO_2}/(\nu \times F_{VOC,in})$, where $F_{VOC,in}$ is the inlet molar flow rate of VOC ($C_{VOC,in}$ is the corresponding concentration), F_{CO_2} is the outlet molar flow rate of CO_2 and ν is the number of carbon atoms in the VOC molecule (for ethyl acetate, $\nu = 4$, for ethanol, $\nu = 2$ and for toluene, $\nu = 7$).

The total amount of carbon retained in the porous structure of the Cr-NaY catalyst after reaction with toluene was measured by temperature programmed oxidation in air (TPO). After the reaction, the catalyst was cooled in nitrogen to 100 °C. Then, a stream of air was passed and the temperature increased at 10 °C/min up to 500 °C, so that all the coke deposited was converted into CO_2/CO and detected by the CO_2/CO analyzers.

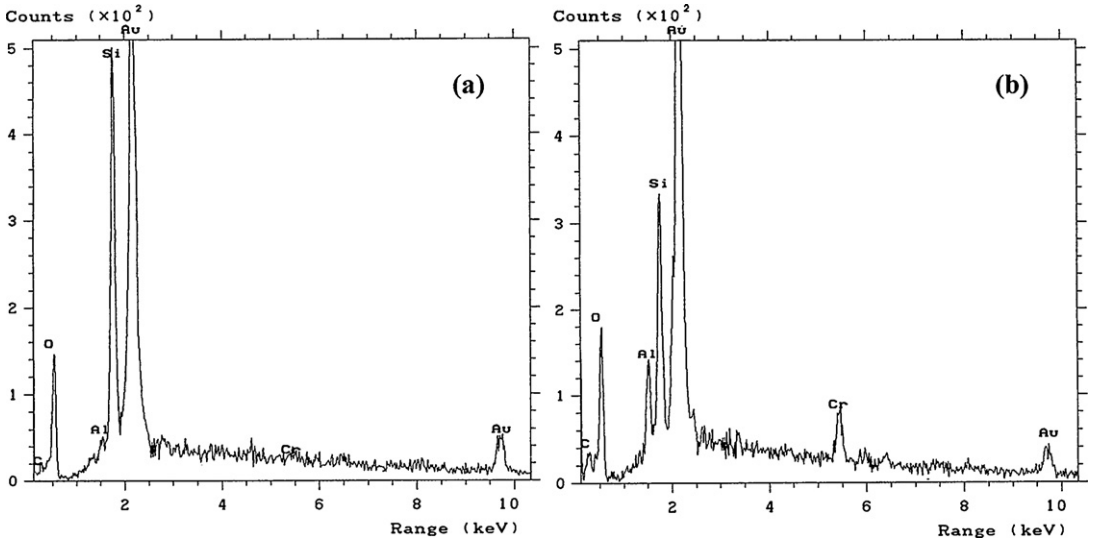

Fig. 1. EDS analysis of Cr-NaY samples obtained at pH 2 (a) and pH 4 (b).

3. Results and discussion

3.1. Biosorption assays

The results of biosorption assays were well discussed in previous work (unpublished). The reduction of Cr(VI) to Cr(III) performed by the bacterium was significantly favoured by lower pH values, as it is essential to supply numerous protons to promote the rate of the reduction reaction. Nevertheless, for extremely acidic pH values, in this case pH 1 and pH 2, the structure of the zeolite is probably damaged and this can explain the lower efficiencies of total Cr removal observed for these pH values. The best removal efficiencies of total chromium were obtained for the highest pH values, 3 and 4, 69.5% and 88.6%, respectively. In order to assess the properties and the applicability of these chromium-loaded zeolites obtained by biosorption in the oxidation of VOC, the samples were characterized by several techniques.

3.2. Characterization

3.2.1. Chemical and morphology analysis

The zeolite samples obtained after biosorption of chromium were characterized by chemical analysis (ICP-AES) and scanning electron microscopy coupled with energy dispersive X-ray spectroscopy (SEM-EDS). The results of bulk chemical analyses revealed a high content of chromium in the zeolite, 0.76% and 0.90% for the catalysts obtained at pH 3 and pH 4, respectively. These results are in agreement with the high removal efficiencies attained for these pH values.

The presence of chromium in the zeolite was also detected by EDS analysis. Fig. 1 presents the surface EDS spectra of Cr-NaY zeolites obtained at pH 2 and pH 4.

The EDS spectra of both Cr-NaY zeolites reveal peaks of Si, Al, Cr, Au, O and C. The presence of Si, Al and O peaks are due to the zeolitic matrix composition, while C peak is attributed to the bacterium organic matter. The appearance of Au peaks is a result of the preliminary coating treatment of the samples with this metal. As can be observed in Fig. 1, the high content of chromium detected in the zeolite obtained at pH 4 is in agreement with the results of bulk chemical analyses. For the zeolite sample obtained at pH 2, a low content of chromium is observed in comparison with the one obtained at pH 4. This is probably related with the damages caused on the zeolite structure due to the extremely acidic conditions.

Fig. 2 shows SEM micrographs of NaY and Cr-NaY catalysts after the biosorption at pH 1, pH 2 and pH 4.

The micrograph presented in Fig. 2(b) shows that the morphology of the catalyst obtained after biosorption at pH 4 did not change in comparison to the starting NaY zeolite. The average particle size of the zeolite obtained at pH 4 and of the starting NaY was about 0.6–0.8 μm. However, the biosorption process performed at very acid pH values such as pH 1 and pH 2 led to changes in the morphology of the zeolites. The external surface of the catalysts obtained at these low pH values seems to become more irregular and rougher. It is also possible to observe a decrease in the particle size of the zeolite as the pH decreases. The catalysts obtained at pH 1 and pH 2 presented a range of particle sizes of about 0.4–0.6 μm and 0.4–0.8 μm, respectively. The damages on the surface structure when severe experimental conditions are used can impart a negative effect on the further utilization of these catalysts for oxidation reactions.

3.2.2. XRD

The XRD patterns of the catalysts prepared at different pH values are illustrated in Fig. 3. It can be seen that the diffraction spectrum of the catalyst obtained at pH 4 is similar to that of the starting NaY zeolite, even though some loss of the intensities of the peaks is observed. This similarity indicates a comparative crystallinity of FAU zeolite phase after the loading of Cr. Nevertheless, the significant loss of intensity and the disappearance of several reflection peaks in the XRD spectra of the samples obtained at lower pH is an evidence of extensive damage in the zeolite structure. This damage became more significant with the decreasing of pH. No diffraction peaks assigned to Cr species occur for any of the catalysts, even at a high Cr loading of 0.9%. Such absence suggests a high dispersion of Cr through the zeolite.

Table 1 summarizes the structural properties obtained by XRD patterns of the starting NaY zeolite and the different catalysts. The unit cell parameters (a_0) were calculated from the [5 3 3], [6 4 2] and [5 5 5] reflection peak positions that were determined using the [1 0 1] reflection of quartz ($2\theta = 26.64187^\circ$) as an internal standard by ASTM D 3942-80. The results reveal that the a_0 lattice parameter was practically unaffected for the catalyst obtained at pH 4, showing at most a decrease of 0.08%, but for the samples obtained at pH 2 and pH 1 a significant decrease of this parameter, 0.24% and 1.79%, respectively, was observed. The relative crystallinity was estimated by comparing the peak intensities of the catalyst sam-

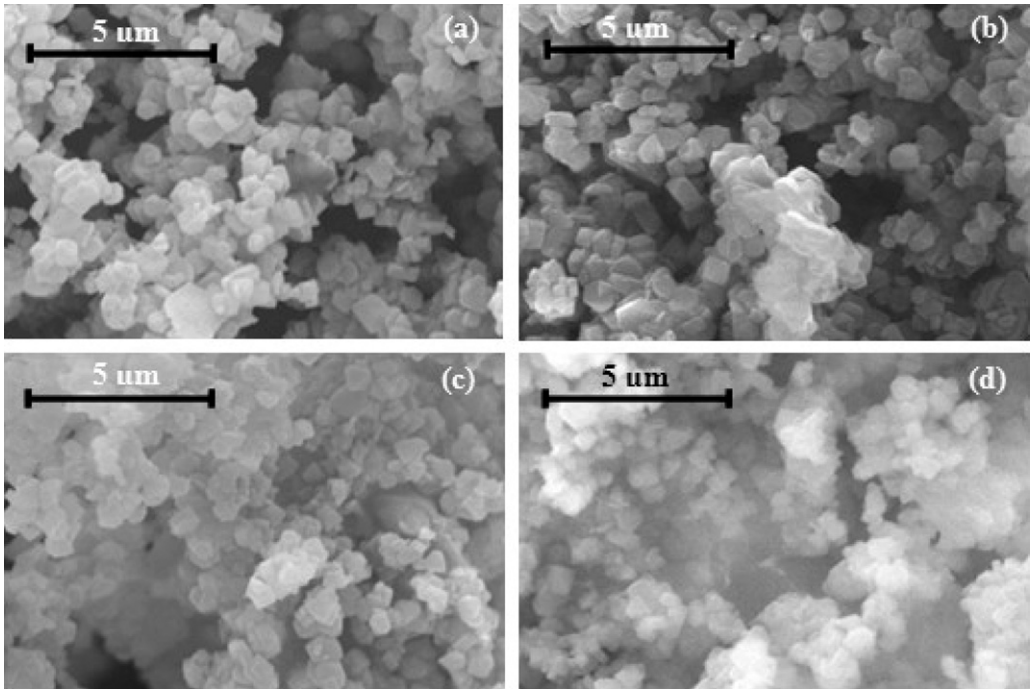

Fig. 2. SEM photograph of the starting NaY zeolite (a), and Cr-NaY zeolites obtained at pH 4 (b), pH 2 (c) and pH 1 (d).

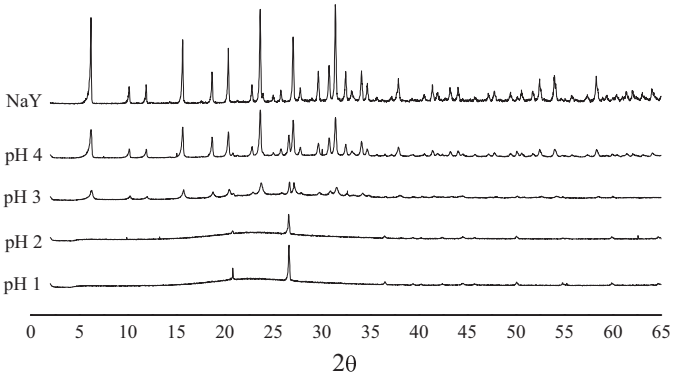

Fig. 3. XRD patterns of NaY and of zeolite samples, obtained at pH 1, pH 2, pH 3 and pH 4.

ples with those of starting NaY (100% of crystallinity). It is possible to observe that the crystallinity significantly decreases as the pH decreases. For the samples obtained at the lower pH values, pH 1 and pH 2, the loss of crystallinity was above 95%. It can also be seen that the molar Si/Al ratio of the samples determined by chemical analysis increased as the solution pH decreases, which indicates the dealumination of the structure catalyzed by the protons in solution.

Table 1
Structural and chemical analyses of catalysts.

Sample	a_0 (Å)[a]	Relative crystallinity (%)[b]	Si/Al_{bulk}[c]
NaY	24.63	100	2.80
Cr-NaY (pH 4)	24.61	68.0	2.95
Cr-NaY (pH 3)	24.57	21.6	3.37
Cr-NaY (pH 2)	24.19	4.1	–
Cr-NaY (pH 1)	–	0.9	–

[a] a_0 is the unit cell parameter determined from XRD analysis.
[b] Comparison with NaY by XRD analysis.
[c] Bulk Si/Al ratio determined by ICP-AES.

3.2.3. Raman

Additional structural information was obtained by Raman spectroscopy. This technique together with XPS provided the identification of chromium species present in these systems. The micro Raman spectra of Cr-NaY obtained from biosorption method at pH 4 are presented in Fig. 4. It was not possible to obtain the Raman spectra of the starting NaY zeolite as this sample showed intense fluorescence which is typically four orders of magnitude more intense than the Raman signal, the latter being overwhelmed by fluorescence.

The Raman spectra of the catalyst show essentially Cr(VI) species. Upon dehydration, a slight shift of the bands that appear in the spectrum of the hydrated sample can be observed. The presence of chromium was observed at bands 980 and 936 cm^{-1} that are related to surface Cr(VI) species. The presence of these species could be related to the calcination conditions that favour the oxidation of Cr(III) to Cr(VI). The bands observed are related to the stretching mode of the terminal Cr=O of surface Cr(VI) species that appear typically at 1007–980 cm^{-1}. In general, as Na coordinates to

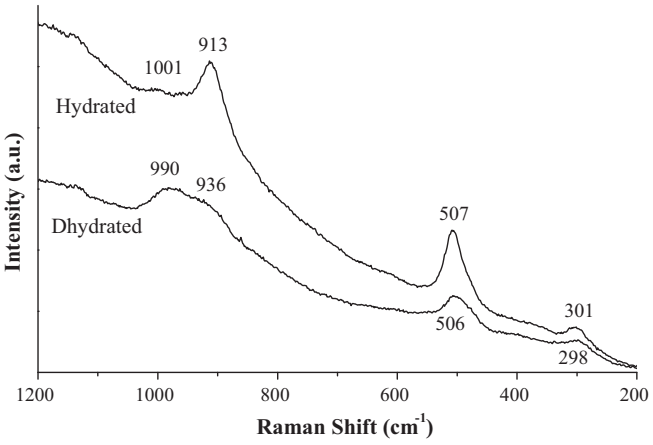

Fig. 4. Raman spectra of Cr-NaY catalyst obtained at pH 4.

Table 2
Elemental analysis determined by XPS.

Sample	XPS (atom%)					Si/Al
	N	C	Si	Al	Cr	
NaY	–	–	23.8	7.4	–	3.10
Cr-NaY (pH 4) calcined	–	6.0	22.0	7.2	0.7	3.06
Cr-NaY (pH 4) uncalcined	4.6	46.2	10.9	3.3	0.7	3.30

surface chromates the Cr=O mode vibration shifts to lower frequencies, and as surface chromate polymerizes the 1007 cm^{-1} band also shifts to lower frequencies and new bands appear at 980–800 cm^{-1} [39]. The Raman bands observed between 200 and 600 cm^{-1} are attributed to the motion of the oxygen atom in a plane perpendicular to the T–O–T bonds in the zeolite structure, which is not sensitive to hydration. The high frequency Raman bands in the range 1100–1200 cm^{-1} are assigned to the asymmetric stretching vibration of the Si–O bond. These Raman bands have mostly low to moderate intensity [40].

3.2.4. XPS

Table 2 presents the XPS analysis based on C 1s, N 1s, Na 1s, Al 2p, Si 2p and Cr 2p peak intensities for NaY and catalyst Cr-NaY (pH 4), before and after calcination. The XPS spectra revealed the presence of sodium, silicon and aluminium for all samples. Carbon and nitrogen from the organic matter of the bacterium before calcination were also detected. The sample exhibits the same content of chromium, 0.7%, at the zeolite surface, before and after calcination. The concentration of chromium determined by XPS is of the same order as that obtained by chemical analysis (0.9%) which is an indication that the metal is uniformly distributed on the zeolite surface. The presence of chromium was detected in the modified zeolite spectrum. The difference between the Si/Al ratios determined on the surface by XPS (Table 2) and those determined in bulk by chemical analysis (Table 1) indicates an uneven distribution of silicon and aluminium throughout the zeolite structure.

The binding energies of the peaks in the Cr 2p region were obtained for the catalyst prepared at pH 4, before and after calcination (Table 3). Before calcination, a significant band appeared at a binding energy of 577.3 eV that corresponds to a Cr $2p_{3/2}$ orbital. After calcination, the spectrum showed two bands at 578.2 eV and 587.7 eV, the former corresponding to a Cr $2p_{3/2}$ orbital and the latter to a Cr $2p_{1/2}$ orbital. In reference compounds the Cr $2p_{3/2}$ orbitals are assigned at 577.2 eV ($CrCl_3$) and 576.2–576.5 eV (Cr_2O_3) for Cr(III) compounds, while Cr(VI) forms are characterized by higher binding energies such as 578.1 eV (CrO_3) or 579.2 eV ($K_2Cr_2O_7$) [41,42]. Boucetta et al. verified that the Cr $2p_{1/2}$ orbitals for Cr(VI) species are assigned in the range 587.6–589.2 eV [43]. Therefore, it can be clearly concluded that chromium loaded in the zeolite is in the trivalent form before calcination and in hexavalent form after calcination, which is consistent with the absence of the Cr_2O_3 sharp Raman band at 550 cm^{-1}. Thus, upon calcination in air, the exchanged Cr(III) suffered oxidation to Cr(VI) species.

3.2.5. H_2-TPR

A TPR experiment was carried out in order to determine the reducibility of chromium in calcined Cr-NaY catalyst (pH 4) and the results are presented in Fig. 5. The H_2-TPR spectrum showed a single broad peak centered at 460 °C. According to several authors [43–47] this consumption of hydrogen could be assigned to Cr(VI) → Cr(III) reduction transitions of chromium species on the zeolite surface. This result is confirmed by the sample colour shift from yellow to light green after the TPR experiment. These observations are an additional indication that oxidation of chromium (initially ion-exchanged as Cr^{3+}) to Cr^{6+} has occurred upon calcination.

Table 3
XPS data of Cr-NaY catalyst obtained at pH 4.

Sample	Cr level	BE (eV)	Oxidation state
Cr-NaY (pH 4) uncalcined	$2p_{3/2}$	577.3	Cr(III)
Cr-NaY (pH 4) calcined	$2p_{3/2}$	578.2	Cr(VI)
	$2p_{1/2}$	587.7	Cr(VI)

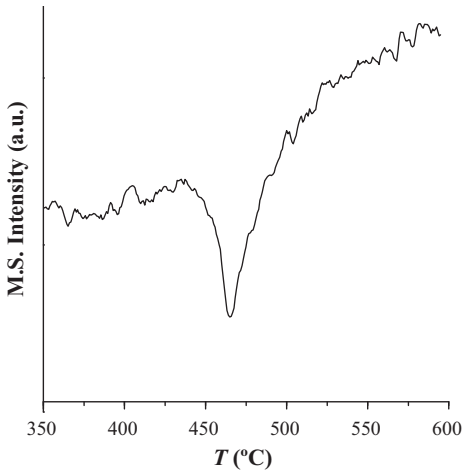

Fig. 5. H_2-TPR spectra of calcined Cr-NaY catalyst (pH 4).

3.2.6. N_2 adsorption

The results of N_2 adsorption isotherms are listed in Table 4. It is clear that the pH is an important parameter in the preparation of catalysts, since it has a significant effect on their textural properties. It can be seen that very acidic conditions lead to a significant decrease of the catalyst surface area and pore volume, which allows foreseeing a worse catalytic performance on the oxidation reactions.

The results of all the characterization techniques allowed to choose the catalyst obtained at pH 4 as the most suitable for VOC oxidation.

3.3. Catalytic tests

The catalytic performance of the Cr-NaY zeolite obtained at pH 4 was evaluated in the oxidation of ethyl acetate, ethanol and toluene. The same study was carried out with the starting NaY zeolite in order to assess the effect of chromium in the catalytic activity.

The light-off curves of a standard experiment consisted in two cycles of: increasing temperature, keeping the temperature constant for 1 h and decreasing it. For all VOC tested, it was observed that the catalytic performance in the increasing temperature step in the first and second cycle was quite similar and the same was observed for the decreasing temperature step. This is a clear indication of the stability of the catalyst in the oxidation reaction. The performance of all catalysts was always compared using the decreasing temperature step.

Table 4
Catalyst characterization by nitrogen adsorption.

Sample	S_{BET} (m^2/g)	$V_{micropore}$ [a] (cm^3/g)	V_p [b] (cm^3/g)
NaY	787	0.347	0.382
Cr-NaY (pH 4)	733	0.308	0.355
Cr-NaY (pH 3)	439	0.185	0.260
Cr-NaY (pH 1)	86	0.043	0.086

[a] Calculated by the t-method.
[b] Total pore volume determined from the amount adsorbed at $P/P_0 = 0.99$.

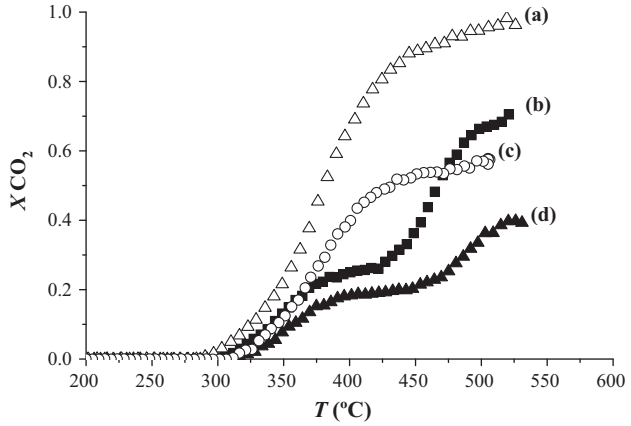

Fig. 6. Light-off curves for the oxidation of ethyl acetate on Cr-NaY and NaY, for the cooling step, at two VOC concentrations: (a) Cr-NaY, 2000 mg_C/m^3 (b) NaY, 2000 mg_C/m^3, (c) Cr-NaY, 4000 mg_C/m^3 and (d) NaY, 4000 mg_C/m^3.

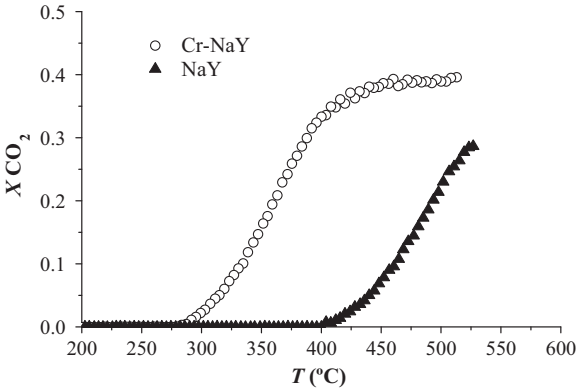

Fig. 7. Light-off curves for the oxidation of ethanol on Cr-NaY and NaY, for the cooling step.

The comparison of the catalytic performance of Cr-NaY catalyst and the starting zeolite, NaY, for the oxidation of ethyl acetate at two different concentrations, 4000 mg_C/m^3 and 2000 mg_C/m^3, is shown in Fig. 6.

Over the Cr-NaY catalyst, the complete oxidation of ethylacetate occurs at 520 °C when the concentration is 2000 mg_C/m^3. For the same VOC concentration and temperature, the maximum conversion into CO_2 for the starting NaY zeolite was only 70%. The presence of chromium in the zeolite allowed a marked decrease of about 85 °C in the temperature required to achieve 50% of CO_2 conversion (T_{50}). When the ethyl acetate concentration was increased from 2000 mg_C/m^3 to 4000 mg_C/m^3, the maximum yield of CO_2 decreased from 100% to 57% for Cr-NaY and from 70% to 40% for NaY, at 520 °C. These results are an indication that probably the catalyst surface is completely covered by ethyl acetate molecules at a concentration of 2000 mg_C/m^3, as the maximum CO_2 conversion decreased by almost half when the concentration was doubled. Therefore, for concentrations above this value, the maximum conversion into CO_2 decreases. Abdullah et al. [48] studied the catalytic activity of a chromium exchanged ZSM-5 zeolite (Cr-ZSM-5) in the decomposition of ethyl acetate, using a similar chromium loading of 0.98% and a higher space velocity of 32 000 h^{-1}, in comparison to the conditions used in this work. These authors obtained a yield of CO_2 of about 80% at 500 °C, while in this study the same conversion was achieved at 420 °C.

The light-off curve of the starting NaY zeolite has two levels in which the conversion into CO_2 remained constant, the first one between 385 °C and 415 °C and the second one starting at 505 °C. The shape of this curve is an indication of the formation and subsequent oxidation of by-products. The absence of the first level in the Cr-NaY light-off curve reveals that the presence of chromium increases not only the activity and selectivity of the catalyst, but also shifts the reaction pathways. However, it should be noted that up to about 300 °C both catalysts have similar performance, and thus chromium does not seem to have an important role at temperatures below this value.

For both catalysts, ethyl acetate conversion (figures not shown) starts at 275 °C, for an ethyl acetate concentration of 2000 mg_C/m^3. Complete conversion of ethyl acetate was achieved with Cr-NaY catalyst at 380 °C, while conversion was only 82% with NaY at 500 °C. It is also important to know the by-products that are formed and if any of these are more harmful than the reactant. The VOC analyzer used in this work (MiniRAE2000) allows the determination of the total amount of VOC but not the identification of the different organic compounds. In order to identify the by-products that are produced, the effluent gas was analyzed by a gas chromatograph equipped with a flame ionization detector (FID). With Cr-NaY, ethylene started to be produced at 275 °C, while CO_2 was formed only above 300 °C, which means that ethyl acetate was initially converted in to ethylene, the latter being converted into CO_2 at temperatures higher than 300 °C. With NaY zeolite, ethylene and CO_2 were simultaneously produced at 300 °C. In this case, part of ethyl acetate is converted directly to CO_2 and the other part is oxidized to ethylene. At 370 °C, a second by-product was produced on NaY, this product being converted at temperatures above 415 °C, which is the starting temperature of the second stage of increasing of CO_2 conversion. This side-product was detected by the total VOC analyzer, but it was not possible to identify this compound by GC. Recently, several authors reported that the catalytic oxidation of ethyl acetate includes several consecutive and/or parallel steps. The first one regards ethyl acetate decomposition to smaller organic molecules, such as ethanol and/or ethylene. The second one consists their further partial oxidation to acetaldehyde or acetic acid and at last, a complete oxidation of these products to CO_2 and H_2O occurs [14,49,50]. Therefore, the unknown by-product formed can probably be acetic acid resulting from the oxidation of ethylene, as this compound is very difficult to detect by GC. With NaY zeolite, the production of CO at 520 °C was also detected.

The catalytic performances of Cr-NaY and the starting NaY zeolite for the oxidation of ethanol were evaluated. The light-off curves obtained are presented in Fig. 7.

It can be observed that complete conversion into CO_2 was not achieved with any of the catalysts tested. The maximum conversion attained with Cr-NaY zeolite was 39% at 450 °C, while the conversion into CO_2 only reached 28% at 520 °C with the starting NaY zeolite. It is clear that the presence of chromium in the zeolite increased dramatically the activity. In terms of comparison, the conversion into CO_2 is about 28% at 380 °C with Cr-NaY, which is 140 °C lower than the required temperature for NaY to reach the same conversion.

With both catalysts, ethanol starts to be converted (data not shown) at temperatures near 140 °C. The complete oxidation of ethanol occurs at 385 °C in the presence of Cr-NaY, while the maximum conversion obtained with NaY was 33% at 410 °C. When Cr-NaY is used as catalyst, acetaldehyde starts to be produced at 140 °C, being converted into a second by-product at temperatures between 220 °C and 270 °C (not detected by GC analysis). At this temperature range acetaldehyde is probably oxidized to the respective carboxylic acid, i.e., acetic acid, according to the reaction pathways for the oxidation of primary alcohols that were reported in several works [18,51]. At 280 °C, ethylene starts to be produced as a result of the dehydration of ethanol and at temperatures higher than 290 °C, the formation of CO_2 and CO occurs as a result of the complete oxidation of the intermediate products. Gucbilmez et al.

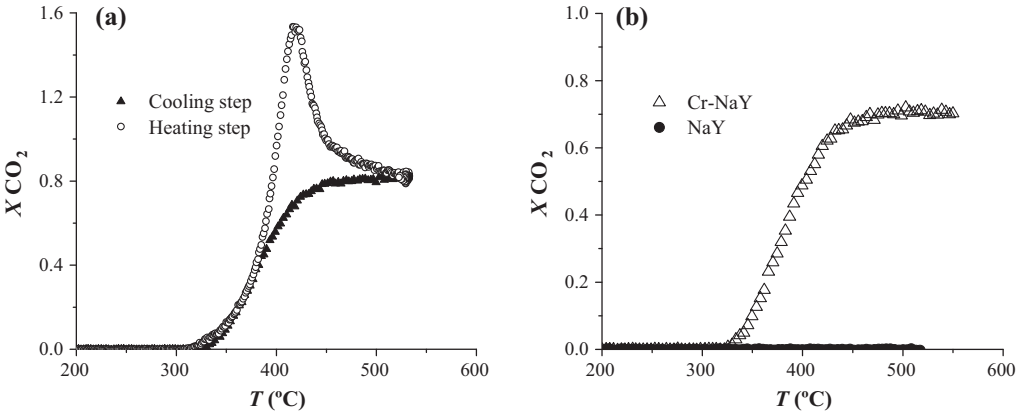

Fig. 8. Light-off curves for the oxidation of toluene on Cr-NaY for the heating and cooling steps (a) and comparison with the performance of NaY catalyst (cooling step) (b).

(2006) also reported the production of ethylene during the oxidation of ethanol over V-MCM-41 catalysts at temperatures between 200 °C and 400 °C [52].

Traces of acetaldehyde were produced at lower temperatures (T < 200 °C) with the starting NaY zeolite, but the main product found was ethylene, at higher temperatures. Ethylene starts to be formed at 250 °C, being converted into CO at 325 °C, which is further converted into CO_2 at temperatures above 405 °C.

In Fig. 8 is shown the light-off curves for toluene oxidation on Cr-NaY, in terms of CO_2 conversion, for the heating and cooling step, and the comparison with the performance of the starting NaY zeolite.

A peak of CO_2 is observed in Fig. 8(a), with conversions higher than 100% between the temperatures of 400 °C and 450 °C. This result can be explained by the adsorption properties of the zeolite and the reactivity of the Cr-NaY catalyst. In this context, it is important to refer the work of Paulis et al. [53]. These authors studied the influence of adsorption and desorption processes in the oxidation of toluene and acetone over Pd/Al_2O_3, Mn_2O_3/Al_2O_3 and Mn_2O_3/SiO_2 catalysts. The light-off curves obtained showed apparent conversions into CO_2 which are higher than 100%, and these results were attributed to the accumulation of coke at low temperatures. Tsou et al. [54,55] have reported an oscillatory behaviour in the oxidation of some VOC compounds over zeolite-based catalysts. The authors found that this phenomenon was due to the adsorption properties of the support and also to the accumulation of coke. In particular, a support which is capable of retaining the VOC at temperatures higher than the reaction temperature can lead to oscillations in the apparent conversion into CO_2. In the present work, the formation of coke during the oxidation of toluene over Cr-NaY zeolite will be further evaluated.

Analyzing Fig. 8(b) it is clear that the presence of chromium in the zeolite dramatically changes the catalytic performance in the oxidation of toluene. With Cr-NaY, the maximum conversion into CO_2 attained was 70% at 450 °C, while the production of CO_2 was not observed at any temperature in the range with the starting NaY zeolite. In terms of VOC conversion (data not shown), toluene started to be converted at 140 °C with Cr-NaY and at 120 °C with NaY. The complete conversion of toluene was achieved at 450 °C with Cr-NaY, whereas the starting zeolite only attained 23% of conversion at 500 °C. With NaY, benzaldehyde starts to be produced at 120 °C and is further converted into CO at temperatures higher than 210 °C. With Cr-NaY, toluene is initially converted into CO at temperatures higher than 140 °C and probably into carbonaceous compounds (coke), as the production of CO_2 only started at 325 °C. Similar results were obtained by Ribeiro et al. [56] for the oxidation of toluene over copper and cesium exchange Y zeolites. These authors used a toluene concentration of 800 ppmv (3000 mg_C/m^3), 300 mg of catalyst and a space velocity of 24 200 h^{-1}. The complete oxidation of toluene occurs at about 450 °C and the maximum CO_2 yield obtained was 80% at 500 °C. Other authors studied toluene oxidation over chromium-based catalysts and obtained a worse performance in terms of activity and selectivity in comparison with this work. Subrahmanyam et al. used Cr-MCM-48 catalysts and obtained a toluene conversion of 11.3% at 375 °C, the main reaction products being benzaldehyde, benzene, CO_2 and CO [57].

The formation of coke on Y zeolites during the oxidation of aromatic compounds was reported by several authors that showed that the acidic sites of the zeolites play a significant role in the formation of carbonaceous compounds [56,58,59]. In order to evaluate the formation of coke in Cr-NaY, TPO analyses were carried out after 1 h reaction with toluene at selected temperatures, 400 °C and 500 °C (Fig. 9). For the reaction at 400 °C, a single broad peak was observed between 360 °C and 500 °C, with a maximum at 440 °C. It is observed that the production of CO_2 (expressed as mass of carbon per 100 g of catalyst, per minute) started at 360 °C, which is 35 °C higher than the temperature at which the formation of CO_2 in the oxidation reaction started. This broad peak is an indication that CO_2 production is not only due to oxidation of toluene molecules adsorbed in the zeolite, but also of carbonaceous compounds resulting from side reactions during the oxidation of toluene. The burning temperature of these compounds is not much higher than the temperature at which toluene total oxidation occurs, which is an indication that probably the compounds are small polymers, such as carbonaceous oligomers. By the integration of the curve, the amount of carbonaceous compounds in the zeolite after 1 h reaction at 400 °C was calculated as 2.25 $g_C/100\ g_{cat}$. On the other hand, after

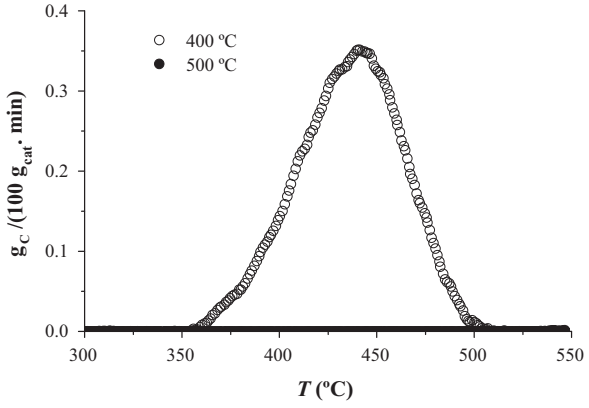

Fig. 9. Temperature programmed oxidation (TPO) after the oxidation of toluene over Cr-NaY catalyst at 400 °C and 500 °C.

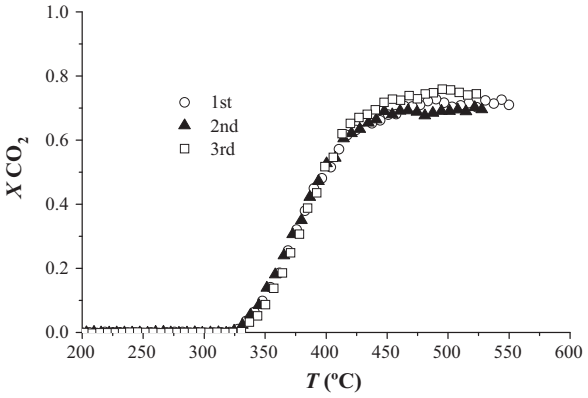

Fig. 10. Reutilization cycles of Cr-NaY catalyst in the oxidation of toluene.

Table 5
Temperatures corresponding to 100% of VOC conversion (T_{100}) and maximum CO_2 yield.

VOC	$T_{100\%}$ (°C)	X_{CO_2} (%)	T (°C)
Ethyl acetate	385	100	520
Ethanol	355	39	450
Toluene	450	70	450

reaction at 500 °C, the production of CO_2 or CO was not observed during the TPO experiment, which means that neither toluene adsorption nor formation of carbonaceous side products occurs at this temperature.

In order to evaluate the possible loss of activity of the Cr-NaY catalyst due to the formation of carbonaceous oligomers, reutilization tests were performed. Between each reaction, a regeneration treatment was performed at 500 °C, through a stream of air. Fig. 10 shows the light-off curves of three consecutive reutilization reactions, each one consisting of two cycles of heating and cooling steps. As it can be seen, the catalyst had the same performance in all the three reutilization reactions and did not show any loss of activity. This is an indication that the carbonaceous oligomers that are deposited in the zeolite are easily burned at 500 °C during the regeneration treatment of the catalyst.

A comparison of the catalytic performance of Cr-NaY in the oxidation of the three VOC studied was made. Table 5 summarizes the temperatures corresponding to 100% of VOC conversion ($T_{100\%}$) and the maximum conversion into CO_2 (X_{CO_2}), for the oxidation of ethyl acetate, ethanol and toluene. Comparing the VOC tested, toluene was the most resistance to oxidation, as it required temperatures 95 °C and 65 °C higher than ethanol and ethyl acetate, respectively, for 100% of conversion. In terms of VOC conversion, the following sequence was observed: ethanol > ethyl acetate > toluene. However, in terms of selectivity to CO_2, ethyl acetate was the only compound for which total oxidation was achieved, and therefore the sequence changes to ethyl acetate > toluene > ethanol.

4. Conclusions

The Cr-NaY zeolite obtained after biosorption of Cr(VI) was successfully reutilized as catalyst in the oxidation of ethyl acetate, ethanol and toluene. XPS analysis proved that chromium was exchanged by the zeolite as Cr(III) and upon calcination the trivalent chromium suffered oxidation to Cr(VI), which was confirmed by Raman and H_2-TPR. For all VOC tested, the presence of chromium in the zeolite shifted the reaction pathways, allowing a notable increase of activity and selectivity to CO_2, in comparison with the starting zeolite NaY. In terms of VOC conversion the following sequence was observed: ethanol > ethyl acetate > toluene. However, in terms of selectivity to CO_2, ethyl acetate was the only VOC for which total oxidation was attained and therefore the above sequence changes to ethyl acetate > toluene > ethanol.

This work presents a double environmental benefit, as it allows the treatment of chromium-contaminated wastewater and simultaneously the removal of VOC from gaseous streams.

Acknowledgments

Dr. C.S. Rodriguez (C.A.C.T.I., Vigo University, Spain) is gratefully acknowledged for performing and interpreting the XPS analyses. Bruna Silva, Hugo Figueiredo and Vera P. Santos thank FCT-Portugal (Fundação para a Ciência e Tecnologia) for the concession of their PhD grants. Anna E. Lewandowska thanks the Spanish Ministry of Science and Innovation for a "Juan de la Cierva" postdoctoral position.

This work was partially funded by the Centre of Biological Engineering and Centre of Chemistry (University of Minho, Portugal) through a POCTI project (ref: POCTI-SFA-3-686), by the Spanish Ministry of Science and Innovation (CTQ2008-04261/PPQ) and by FCT and FEDER under Programs POCI 2010 and COMPETE, Project PTDC/AMB/69065/2006.

References

[1] R.J. Heinsohn, R.L. Kabel, Source and Control of Air Pollution, Prentice Hall, Upper Saddle River, New Jersey, 1999.
[2] R. Atkinson, Atmospheric chemistry of VOCs and NOx, Atmos. Environ. 34 (2000) 2063–2101.
[3] R.E. Hester, R.M. Harrison, Volatile Organic Compounds in the Atmosphere, Royal Society of Chemistry, 1995.
[4] EU Council Directive 2001/81/EC of 23 October 2001.
[5] M.A. Centeno, M. Paulis, M. Montes, J.A. Odriozola, Catalytic combustion of volatile organic compounds on $Au/CeO_2/Al_2O_3$ and Au/Al_2O_3 catalysts, Appl. Catal. A 234 (2002) 65–78.
[6] A. dos Santos, K. Lima, R. Figueiredo, S. Egues, A. Ramos, Toluene deep oxidation over noble metals, copper and vanadium oxides, Catal. Lett. 114 (2007) 59–63.
[7] R.S.G. Ferreira, P.G.P. de Oliveira, F.B. Noronha, The effect of the nature of vanadium species on benzene total oxidation, Appl. Catal. B 29 (2001) 275–283.
[8] V. Gaur, A. Sharma, N. Verma, Catalytic oxidation of toluene and m-xylene by activated carbon fiber impregnated with transition metals, Carbon 43 (2005) 3041–3053.
[9] S.C. Kim, W.G. Shim, Influence of physicochemical treatments on iron-based spent catalyst for catalytic oxidation of toluene, J. Hazard. Mater. 154 (2008) 310–316.
[10] R. Rachapudi, P.S. Chintawar, H.L. Greene, Aging and structure/activity characteristics of Cr-ZSM-5 catalysts during exposure to chlorinated VOCs, J. Catal. 185 (1999) 58–72.
[11] C.-H. Wang, S.-S. Lin, C.-L. Chen, H.-S. Weng, Performance of the supported copper oxide catalysts for the catalytic incineration of aromatic hydrocarbons, Chemosphere 64 (2006) 503–509.
[12] C.T. Wong, A.Z. Abdullah, S. Bhatia, Catalytic oxidation of butyl acetate over silver-loaded zeolites, J. Hazard. Mater. 157 (2008) 480–489.
[13] E.C. Moretti, Reduce VOC and HAP emissions, Chem. Eng. Prog. 98 (2002).
[14] P.-O. Larsson, A. Andersson, Complete oxidation of CO, ethanol, and ethyl acetate over copper oxide supported on titania and ceria modified titania, J. Catal. 179 (1998) 72–89.
[15] C.-Y. Lu, M.-Y. Wey, Simultaneous removal of VOC and NO by activated carbon impregnated with transition metal catalysts in combustion flue gas, Fuel Process. Technol. 88 (2007) 557–567.
[16] P. Papaefthimiou, T. Ioannides, X.E. Verykios, Catalytic incineration of volatile organic compounds present in industrial waste streams, Appl. Therm. Eng. 18 (1998) 1005–1012.
[17] V.H. Vu, J. Belkouch, A. Ould-Dris, B. Taouk, Removal of hazardous chlorinated VOCs over Mn–Cu mixed oxide based catalyst, J. Hazard. Mater. 169 (2009) 758–765.
[18] G. Avgouropoulos, E. Oikonomopoulos, D. Kanistras, T. Ioannides, Complete oxidation of ethanol over alkali-promoted Pt/Al_2O_3 catalysts, Appl. Catal. B 65 (2006) 62–69.
[19] F.J. Maldonado-Hódar, C. Moreno-Castilla, A.F. Pérez-Cadenas, Catalytic combustion of toluene on platinum-containing monolithic carbon aerogels, Appl. Catal. B 54 (2004) 217–224.
[20] V.P. Santos, S.A.C. Carabineiro, P.B. Tavares, M.F.R. Pereira, J.J.M. Órfão, J.L. Figueiredo, Oxidation of CO, ethanol and toluene over TiO_2 supported noble metal catalysts, Appl. Catal. B 99 (2010) 198–205.
[21] J. Tsou, P. Magnoux, M. Guisnet, J.J.M. Órfão, J.L. Figueiredo, Catalytic oxidation of volatile organic compounds: oxidation of methyl-isobutyl-ketone over Pt/zeolite catalysts, Appl. Catal. B 57 (2005) 117–123.

[22] V.P. Santos, M.F.R. Pereira, J.J.M. Órfão, J.L. Figueiredo, The role of lattice oxygen on the activity of manganese oxides towards the oxidation of volatile organic compounds, Appl. Catal. B 99 (2010) 353–363.
[23] V.H. Vu, J. Belkouch, A. Ould-Dris, B. Taouk, Catalytic oxidation of volatile organic compounds on manganese and copper oxides supported on titania, AIChE J. 54 (2008) 1585–1591.
[24] Y. Yang, X. Xu, K. Sun, Catalytic combustion of ethyl acetate on supported copper oxide catalysts, J. Hazard. Mater. 139 (2007) 140–145.
[25] V.P. Santos, S.S.T. Bastos, M.F.R. Pereira, J.J.M. Órfão, J.L. Figueiredo, Stability of a cryptomelane catalyst in the oxidation of toluene, Catal. Today 154 (2010) 308–311.
[26] R. López-Fonseca, J. Gutiérrez-Ortiz, M. Gutiérrez-Ortiz, J. González-Velasco, Catalytic combustion of chlorinated ethylenes over H-zeolites, J. Chem. Technol. Biotechnol. 78 (2003) 15–22.
[27] J.J. Spivey, J.B. Butt, Literature review: deactivation of catalysts in the oxidation of volatile organic compounds, Catal. Today 11 (1992) 465–500.
[28] C. Lahousse, A. Bernier, P. Grange, B. Delmon, P. Papaefthimiou, T. Ioannides, X. Verykios, Evaluation of gamma-MnO_2 as a VOC removal catalyst: comparison with a noble metal catalyst, J. Catal. 178 (1998) 214–225.
[29] G. Mata, R. Trujillano, M.A. Vicente, C. Belver, M. Fernández-García, S.A. Korili, A. Gil, Chromium-saponite clay catalysts: preparation, characterization and catalytic performance in propene oxidation, Appl. Catal. A 327 (2007) 1–12.
[30] H. Rotter, M.V. Landau, M. Carrera, D. Goldfarb, M. Herskowitz, High surface area chromia aerogel efficient catalyst and catalyst support for ethylacetate combustion, Appl. Catal. B 47 (2004) 111–126.
[31] M. Kang, C.-H. Lee, Methylene chloride oxidation on oxidative carbon-supported chromium oxide catalyst, Appl. Catal. A 266 (2004) 163–172.
[32] H.L. Tidahy, S. Siffert, F. Wyrwalski, J.F. Lamonier, A. Aboukaïs, Catalytic activity of copper and palladium based catalysts for toluene total oxidation, Catal. Today 119 (2007) 317–320.
[33] B. Silva, H. Figueiredo, C. Quintelas, I.C. Neves, T. Tavares, Zeolites as supports for the biorecovery of hexavalent and trivalent chromium, Microporous Mesoporous Mater. 116 (2008) 555–560.
[34] H. Figueiredo, I.C. Neves, C. Quintelas, T. Tavares, M. Taralunga, J. Mijoin, P. Magnoux, Oxidation catalysts prepared from biosorbents supported on zeolites, Appl. Catal. B 66 (2006) 274–280.
[35] D. Eaton, L.S. Clesceri, A.E. Greenberg, Standard Methods for the Examination of Water and Wastewater, American Public Health Association (APHA), Washington, 1995.
[36] J.F. Moulder, W.F. Strickle, P.E. Sobol, K.D. Bomben, Handbook of X-ray Photoelectron Spectroscopy, Perkin-Elmer, Minnesota, 1992.
[37] Y. Xie, P.M.A. Sherwood, X-ray photoelectron-spectroscopic studies of carbon fiber surfaces. 11. Differences in the surface chemistry and bulk structure of different carbon fibers based on poly(acrylonitrile) and pitch and comparison with various graphite samples, Chem. Mater. 2 (1990) 293–299.
[38] S.S.T. Bastos, J.J.M. Órfão, M.M.A. Freitas, M.F.R. Pereira, J.L. Figueiredo, Manganese oxide catalysts synthesized by exotemplating for the total oxidation of ethanol, Appl. Catal. B 93 (2009) 30–37.
[39] J.E. Maslar, W.S. Hurst, T.A. Vanderah, I. Levin, The Raman spectra of Cr_3O_8 and Cr_2O_5, J. Raman Spectrosc. 32 (2001) 201–206.
[40] P.-P. Knops-Gerrits, D.E. De Vos, E.J.P. Feijen, P.A. Jacobs, Raman spectroscopy on zeolites, Microporous Mater. 8 (1997) 3–17.
[41] L. Dambies, C. Guimon, S. Yiacoumi, E. Guibal, Characterization of metal ion interactions with chitosan by X-ray photoelectron spectroscopy, Colloids Surf. A 177 (2000) 203–214.
[42] D. Park, Y.-S. Yun, J.M. Park, Reduction of hexavalent chromium with the brown seaweed ecklonia biomass, Environ. Sci. Technol. 38 (2004) 4860–4864.
[43] C. Boucetta, M. Kacimi, A. Ensuque, J.-Y. Piquemal, F. Bozon-Verduraz, M. Ziyad, Oxidative dehydrogenation of propane over chromium-loaded calcium-hydroxyapatite, Appl. Catal. A 356 (2009) 201–210.
[44] A.B. Gaspar, J.L.F. Brito, L.C. Dieguez, Characterization of chromium species in catalysts for dehydrogenation and polymerization, J. Mol. Catal. 203 (2003) 251–266.
[45] K. Hadjiivanov, A. Penkova, R. Kefirov, S. Dzwigaj, M. Che, Influence of dealumination and treatments on the chromium speciation in zeolite CrBEA, Microporous Mesoporous Mater. 124 (2009) 59–69.
[46] L. Liu, H. Li, Y. Zhang, Mesoporous silica-supported chromium catalyst: characterization and excellent performance in dehydrogenation of propane to propylene with carbon dioxide, Catal. Commun. 8 (2007) 565–570.
[47] B.M. Weckhuysen, R.A. Schoonheydt, J.-M. Jehng, I.E. Wachs, S.J. Cho, R. Ryoo, S. Kijlstra, E. Poels, Combined DRS-RS-EXAFS-XANES-TPR study of supported chromium catalysts, J. Chem. Soc., Faraday Trans. 91 (1995) 3245–3253.
[48] A.Z. Abdullah, M.Z.A. Bakar, S. Bhatia, Effect of hydrogen treatment on the performance of Cr-ZSM-5 in deep oxidative decomposition of ethyl acetate and benzene in air, Catal. Commun. 4 (2003) 555–560.
[49] A.R. Gandhe, J.S. Rebello, J.L. Figueiredo, J.B. Fernandes, Manganese oxide OMS-2 as an effective catalyst for total oxidation of ethyl acetate, Appl. Catal. B 72 (2007) 129–135.
[50] T. Tsoncheva, L. Ivanova, R. Dimitrova, J. Rosenholm, Physicochemical and catalytic properties of grafted vanadium species on different mesoporous silicas, J. Colloid Interface Sci. 321 (2008) 342–349.
[51] X. Li, E. Iglesia, Selective catalytic oxidation of ethanol to acetic acid on dispersed Mo–V–Nb mixed oxides, Chem. Eur. J 13 (2007) 9324–9330.
[52] Y. Gucbilmez, T. Dogu, S. Balci, Ethylene and acetaldehyde production by selective oxidation of ethanol using mesoporous V-MCM-41 catalysts, Ind. Eng. Chem. Res. 45 (2006) 3496–3502.
[53] M. Paulis, L.M. Gandía, A. Gil, J. Sambeth, J.A. Odriozola, M. Montes, Influence of the surface adsorption–desorption processes on the ignition curves of volatile organic compounds (VOCs) complete oxidation over supported catalysts, Appl. Catal. B 26 (2000) 37–46.
[54] J. Tsou, P. Magnoux, M. Guisnet, J.J.M. Órfão, J.L. Figueiredo, Oscillations in the oxidation of MIBK over a Pt/HFAU catalyst: role of coke combustion, Catal. Commun. 4 (2003) 651–656.
[55] J. Tsou, P. Magnoux, M. Guisnet, J.J.M. Órfão, J.L. Figueiredo, Oscillations in the catalytic oxidation of volatile organic compounds, J. Catal. 225 (2004) 147–154.
[56] M.F. Ribeiro, J.M. Silva, S. Brimaud, A.P. Antunes, E.R. Silva, A. Fernandes, P. Magnoux, D.M. Murphy, Improvement of toluene catalytic combustion by addition of cesium in copper exchanged zeolites, Appl. Catal. B 70 (2007) 384–392.
[57] C. Subrahmanyam, B. Louis, F. Rainone, B. Viswanathan, A. Renken, T.K. Varadarajan, Catalytic oxidation of toluene with molecular oxygen over Cr-substituted mesoporous materials, Appl. Catal. A 241 (2003) 205–215.
[58] L. Becker, H. Förster, Investigations of coke deposits formed during deep oxidation of benzene over Pd and Cu exchanged Y-type zeolites, Appl. Catal. A 153 (1997) 31–41.
[59] M. Guisnet, P. Dégé, P. Magnoux, Catalytic oxidation of volatile organic compounds. 1. Oxidation of xylene over a 0.2 wt% Pd/HFAU(17) catalyst, Appl. Catal. B 20 (1999) 1–13.